BIOPHYSICS AND BASIC BIOMEDICAL RESEARCH – Full Papers

Magnetic Resonance in Medicine 77:2372–2380 (2017)

EPR Analysis of Extra- and Intracellular Nitric Oxide in Liver Biopsies

Sergiu D. Dumitrescu,[1†] Andras T. Meszaros,[1,2†] Stefan Puchner,[1] Adelheid Weidinger,[1] Mihaly Boros,[2] Heinz Redl,[1] and Andrey V. Kozlov[1]*

Purpose: To develop an assay that can enable the quantification of intra- and extracellular nitric oxide (NO) levels in liver biopsies without application of potentially harmful exogenous NO traps.

Theory: Electron paramagnetic resonance (EPR) spectroscopy is currently the most appropriate method of measuring NO in biological samples due to the outstanding specificity resulting from the interaction of NO with exogenous NO traps. Because such traps are not allowed in clinical settings, we tested the reliability of endogenous NO traps for the determination of NO levels in blood and liver compartments.

Methods: Rats were injected with 0–8 mg/kg lipopolysaccharide (LPS) to gradually induce a systemic inflammatory response. Specific features of NO-hemoglobin and NO–Fe EPR signals were quantified using a specifically developed calibration procedure.

Results: Whereas both NO–hemoglobin ($NO–Hb^{LIVER\ BLOOD}$) and NO–Fe ($NO–Fe^{LIVER}$) complexes were detected in nonperfused liver tissue, only NO–Fe complexes were detected in perfused tissue and only NO–Hb complexes were detected in blood ($NO–Hb^{BLOOD}$). The NO concentrations increased in the sequence $NO–Hb^{BLOOD} < NO–Fe^{LIVER} < NO–Hb^{LIVER\ BLOOD}$ (9.4, 18.5, 27.9 nmol/cm^3, respectively at 2.5 mg/kg LPS). The detection limit of the method was 0.61 nmol/cm^3 for NO–Hb and 0.52 nmol/cm^3 for NO–Fe.

Conclusion: The assay reported here does not influence natural NO pathways and enables the quantification of NO distribution in two liver compartments using a single liver biopsy. **Magn Reson Med 77:2372–2380, 2017. © 2016 International Society for Magnetic Resonance in Medicine**

Key words: endogenous NO traps; mononitrosyl-hemoglobin complex; dinitrosyl–iron complex; nitric oxide; electron paramagnetic resonance

INTRODUCTION

Nitric oxide (NO) is a powerful signaling molecule that regulates some of the most fundamental physiological processes in living organisms, including vascular tone, neurotransmission, host defense systems, and others (1). In mammals, NO is synthesized by a family of enzymes called NO synthases (NOS; EC 1.14.13.39), which includes three isoforms: the constitutively expressed neuronal NOS (NOS I), endothelial NOS (NOS III), and inducible NOS (NOS II). All three isoforms convert L-arginine to L-citrulline and NO in the presence of oxygen.

Neuronal NOS is expressed predominantly in specific neurons of the central nervous system. It regulates gut peristalsis, vasodilation, and penile erection, acts as an atypical neurotransmitter, and has been suggested to partake in memory formation and learning [reviewed by Forstermann and Sessa (2)].

Expression of inducible NOS can be activated by cytokines and other molecules and is crucial for many processes in various cell types, such as defense against bacteria in macrophages (3,4). In addition, the upregulation of inducible NOS occurs in response to inflammation in both parenchymal cells and cells within the blood compartment, implicating several symptoms that are mediated by NO (5).

Endothelial NOS is expressed mostly in endothelial cells (2) but was also found in cardiac myocytes, platelets, specific neurons in the brain, syncytiotrophoblasts in human placenta, and a kidney tubular epithelial cell line [reviewed by Forstermann and Sessa (2)].

An additional pathway of NO formation is the reduction of nitrite by a group of enzymes called nitrite reductases, which, in contrast to NOS, exert higher activity under hypoxia (6). Nitrite reductases are heme proteins located in the blood compartment (hemoglobin [Hb] in red blood cells [RBCs]) and in parenchymal cells of tissues (mitochondria, myoglobin, xanthine oxidoreductase) (6,7). This source of NO is associated with cytoprotective effects and regulation of hemodynamics (6,7).

In general, NO is considered a physiological messenger. However, in addition to physiological functions, NO may be deleterious due to NO-mediated modification of proteins, induction of neurotoxicity, inhibition of mitochondrial respiration, and organelle fragmentation (8). The majority of deleterious effects of NO are associated with the formation of peroxynitrite, a product of the interaction between NO and superoxide. Peroxynitrite formation is typical for immune cells, which are able to destroy microorganisms using the very reactive nature of this molecule (9). NO generated by immune cells in the blood contributes to killing of bacteria and can also cause damage to the host. A part of NO produced in blood is trapped by Hb-forming mononitrosyl–

[1]Ludwig Boltzmann Institute for Experimental and Clinical Traumatology, Vienna, Austria.

[2]Institute of Surgical Research, University of Szeged, Szeged, Hungary.

*Correspondence to: Andrey V. Kozlov, Ph.D., Ludwig Boltzmann Institute for Experimental and Clinical Traumatology, Vienna, Austria.
E-mail: andrey.kozlov@trauma.lbg.ac.at

[†]These authors contributed equally to this work.

Received 2 March 2016; revised 8 May 2016; accepted 9 May 2016

DOI 10.1002/mrm.26291

Published online 1 July 2016 in Wiley Online Library (wileyonlinelibrary.com).

hemoglobin complexes (NO–Hb) (10); another part of NO reacts with oxyhemoglobin and is oxidized to nitrate (11). In contrast, NO produced inside the cells forms predominantly dinitrosyl–iron complexes (NO–Fe) (12). In blood plasma, however, there are no ferrous ions (Fe^{2+}), because they are oxidized by ceruloplasmin and subsequently bound to transferrin. This suggests that these two NO-related signals (NO–Hb and NO–Fe) provide information about intra- and extracellular NO production in organs.

Because the preparation/homogenization of tissue may result in changes of NO levels, we used unprocessed shock frozen liver biopsies which were analyzed by means of low temperature (liquid nitrogen) electron paramagnetic resonance (EPR) spectroscopy.

METHODS

Chemicals

All chemicals were obtained from Sigma-Aldrich (Vienna, Austria) unless noted otherwise.

Animals

The *in vivo* experiments were performed on male Sprague–Dawley rats (n = 45; weight, 250–300/390–540 g; Animal Research Laboratories, Himberg, Austria/Charles River, Germany) which were kept under controlled standard animal housing conditions. The animals had free access to standard laboratory rodent food and water. They were kept for 7 days prior to usage in experiments for accommodation. All interventions were conducted in compliance with the National Institutes of Health's "Guide for the Care and Use of Laboratory Animals" with approval from the Animal Protocol Review Board of the city government of Vienna, Austria.

Lipopolysaccharide Treatment

Lipopolysaccharide (LPS) from *Escherichia coli* serotype 026:B6 (activity ≥500,000 EU/mg) was used for the dose-dependence experiments. Six groups of rats were injected with various doses (0.2, 1.3, 2.5, 4.7, 6.3, and 8.5 mg/kg body weight) of LPS dissolved in saline (Fresenius Kabi, Bad Homburg vor der Höhe, Germany). Control animals were injected with saline only. Samples were collected 16 h after LPS injection.

In a separate set of experiments, animals were divided into five groups. All rats were injected with the same dose of LPS (*Escherichia coli* serotype 026:B6, 8 mg/kg body weight, activity ≥10,000 EU/mg) dissolved in saline, and samples were taken 2, 4, 8, and 16 h after LPS treatment. Control animals were injected with saline only.

The LPS solution was vortexed for 1 min and sonicated for 30 s before application, and subsequently injected in the penis vein under isoflurane anaesthesia in a volume ranging from 0.5 to 0.75 mL.

Design of Animal Experiments and Sampling of Blood and Liver Tissue

In order to prevent unnecessary pain, buprenorphine (Richter Pharma AG, Wels, Austria, 0.05 mg/kg body weight) was injected subcutaneously at the time of LPS treatment and 10 h thereafter.

At the end of the treatment phase with LPS, or to obtain samples for control and calibration purposes, rats were anesthetized via inhalation of a mixture of 3% isoflurane and oxygen. After a small skin cut, the left femoral artery was dissected and catheterized using a 24-gauge intravenous cannula (BD Neoflon; Becton Dickinson Infusion Therapy AB, Helsingborg, Sweden). A total of 10–12 mL whole blood was collected in a 50-mL Falcon tube prefilled with 200 μL of sodium heparin (1000 IU/mL; Gilvasan Pharma GmbH, Vienna, Austria) for subsequent processing and for the *in vitro* part of the study.

For determination of the NO–Hb level, blood samples were taken into Minicollect tubes coated with lithium heparin (Greiner Bio-One GmbH, Kremsmünster, Austria). After centrifugation at 4 °C and 1600 g for 10 min, the plasma was removed and the erythrocyte pellet was collected in 1-mL plastic syringes and subsequently shock-frozen in liquid nitrogen for storage at −80 °C until EPR measurement.

Following the blood sampling, the animals were killed via decapitation. Subsequently, the liver was excised and transferred immediately to a beaker filled with ice-cold Ringer solution (Fresenius Kabi AG, Bad Homburg vor der Höhe, Germany). After cooling down, the liver was cut into small pieces on a Petri dish placed on ice. Tissue samples to a volume of 0.4 mL were filled in 1-mL plastic syringes and shock-frozen in liquid nitrogen and stored at −80 °C for further measurements.

Preparation of Blood and Liver Calibration Samples for EPR

Calibration samples were prepared separately from blood and liver of LPS-untreated animals. For the isolation of blood and liver tissue, the rats were anesthetized as described above and killed via decapitation. Blood (10–15 mL) was collected into a 50-mL Falcon tube that was prefilled with 200 μL of sodium heparin (1000 IU/mL; Gilvasan Pharma GmbH, Vienna, Austria) and placed on ice for cooling. Subsequently, the liver was perfused *in situ* through the portal vein and inferior caval vein, with ice-cold Ringer-sodium heparin solution (0.8 IU sodium heparin/mL Ringer solution) until the effluent solution contained no more blood. After perfusion, the liver was transferred to ice cold Ringer solution.

Collected erythrocytes and liver were used to prepare hemolysates and homogenates, respectively. In order to isolate the RBCs, collected blood was washed twice with ice-cold saline (0.9%), centrifuged at 4°C and 1600 g for 10 min, and separated from supernatant. RBCs were diluted 1:2 with double distilled water and homogenized using an overhead stirrer (RW16, IKA Werke, Staufen im Breisgau, Germany). The concentration of heme in the RBC-hemolysate was determined on the basis of spectrophotometric measurements (350–600 nm; UV-1800, Shimadzu, Kyoto, Japan) and the Soret band corresponding to deoxyhemoglobin. For the preparation of liver homogenates, approximately 2 g of liver tissue were homogenized 1:3 with ice-cold saline (0.9%).

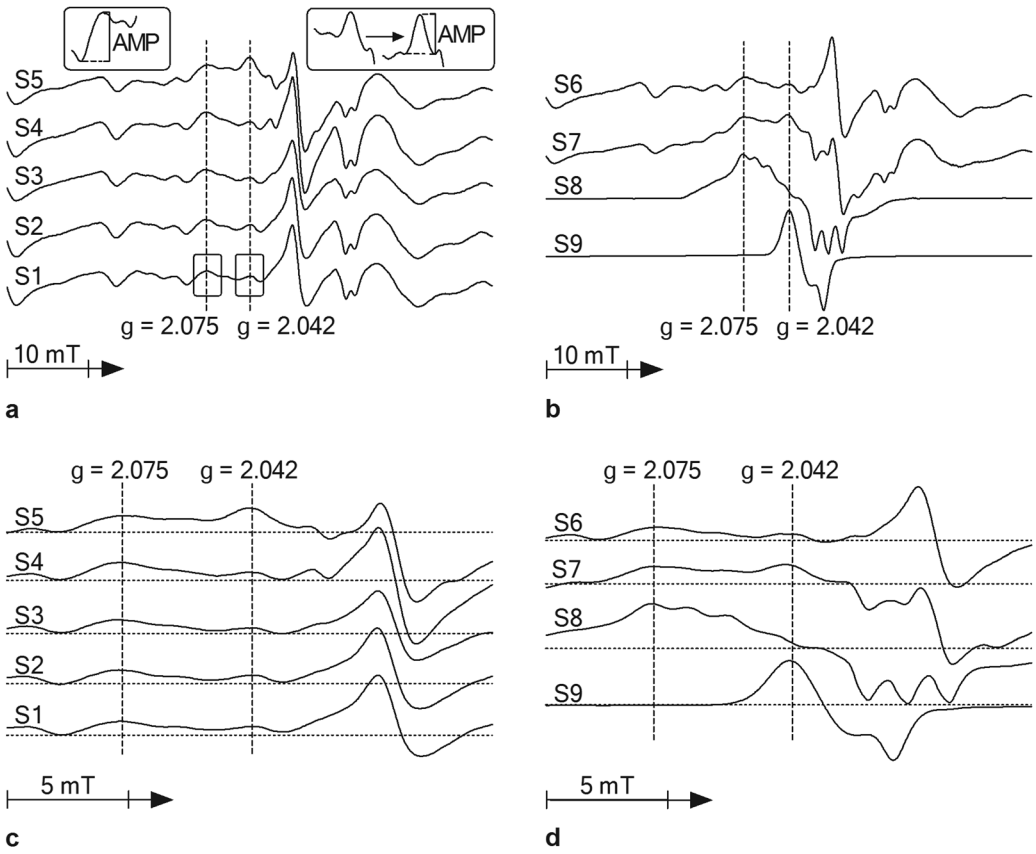

FIG. 1. Complete traces showing the changes in EPR spectra of liver samples obtained from control rats (S1) and from rats 2 (S2), 4 (S3), 8 (S4), and 16 (S5) h after LPS challenge (**a**). The enlarged section of these EPR spectra (**c**) shows two peaks ($g = 2.075$ and $g = 2.042$) increasing in a time-dependent manner. The peak observed at $g = 2.075$ increased within the time frame of 2–8 h (S2–S4), whereas the peak observed at $g = 2.042$ began to increase only after 16 h (S5). To identify these signals, the corresponding full length (**b**) or an enlarged cutout (**d**) of these liver spectra were plotted together with EPR spectra of model mononitrosyl–hemoglobin (NO–Hb, S8) and dinitrosyl–iron (NO–Fe, S9) complexes occurring at the same g-factors. Compared with these very clear spectra, those obtained from sham-operated animals (S6) and animals challenged with 6.3 mg/kg body weight of LPS for 16 h (S7) showed NO–Hb and NO–Fe signals that overlapped with other naturally occurring liver signals. These samples were prepared from either hemolysate or liver homogenate as described in the Methods. Abbreviations: AMP, amplitude; g, g-factor; S, signal.

Preparation of NO–Hb and NO–Fe Complexes for EPR Calibration

EPR samples for NO–Hb and NO–Fe calibration curves were prepared either from RBC–hemolysate or liver homogenate. For NO–Hb calibration, the samples for the calibration curve were prepared in two different ways, resulting in two independent calibration curves. One of these sample series was prepared by mixing hemolysate to final concentrations of heme ranging from 1 to 150 μM and $NaNO_2$ to a final concentration of 1 M. The second sample series was prepared by mixing hemolysate to a final concentration of 5 mM with $NaNO_2$ to final concentrations in a range of 1–150 μM. Regardless of preparation procedure, each sample was prepared in a volume of 500 μL with 50 mg of $Na_2S_2O_4$ to remove the bound oxygen from heme and reduce $NaNO_2$ to NO. The samples for calibration curve of NO–Fe were prepared by mixing liver homogenate with $Fe(II)SO_4$ (final concentration, 1–150 μM) and $NaNO_2$ (concentration, 1 M) to a final volume of 500 μL. Calibration samples were subsequently filled in 1-mL plastic syringes, shock-frozen in liquid nitrogen and stored at −80°C for further measurements.

EPR Measurements

EPR spectra were recorded at liquid nitrogen temperature (−196°C) with a Magnettech MiniScope MS 200 EPR spectrometer (Magnettech, Berlin, Germany) in a quartz finger-type Dewar flask filled with liquid nitrogen. The EPR spectra were recorded at short- and long-scale ranges. The general settings for a short range were as follows: modulation frequency, 100 kHz; microwave frequency, 9.425 GHz; microwave power, 8.3 mW; modulation amplitude, 5 G; and gain, 200. NO–Hb complexes were recorded at 3300 ± 200 G. The general settings for long range were as follows: modulation frequency, 100 kHz; microwave frequency, 9.429 GHz; microwave power, 30 mW; and modulation amplitude, 6 G. Liver spectra were recorded at 3200 ± 500 G. The spectra were quantified by the determination of magnitudes of different components of spectra and by double integration of EPR spectra.

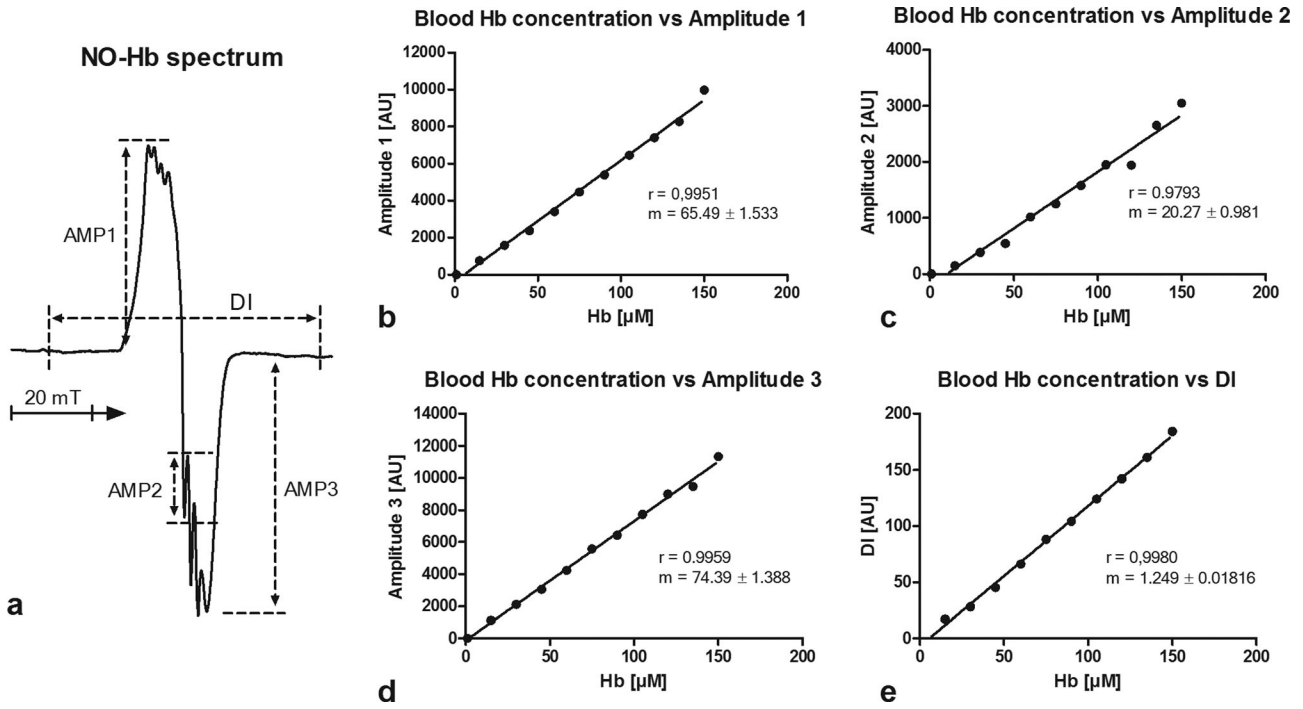

FIG. 2. Calibration of NO–Hb using 1–150 μM Hb, 1 M nitrite, and 50 mg dithionite per sample. The typical EPR spectra recorded in NO–Hb calibration samples (**a**) provide four different quantitative parameters that can be used for the quantification of NO–Hb: AMP1, AMP2, AMP3, and the DI. The concentration of Hb and intensity of NO–Hb signal, which was calculated based on AMP1 (**b**), AMP2 (**c**), AMP3 (**d**), and DI (**e**), show a strong positive correlation. This was observed in case of all quantitative parameters of the spectrum, indicating that any of these parameters can be used for quantification. Abbreviations: AMP, amplitude; m, slope; r, coefficient of determination.

Data Presentation and Statistical Analysis

Statistical evaluation of data was performed using GraphPad Prism 5.01 for Windows (GraphPad Software, La Jolla, California, USA). Statistical significance of correlations was analyzed using Pearson's test.

RESULTS

EPR spectra of rats challenged with LPS showed an increase in the intensity of two peaks located at $g = 2.075$ and $g = 2.042$ (Fig. 1). The signal observed at $g = 2.075$ was already elevated significantly between 2 and 8 h after LPS challenge (Fig. 1a and 1c, S2–S4), whereas the signal at $g = 2.042$ rose only after 16 h after challenge. These signals were identified on the basis of their comparison with the model NO–Hb (Fig. 1b and 1d, S8) and NO–Fe (Fig. 1b and 1d, S9) complexes. In Figure 1b and 1d, EPR signals of model complexes were compared with signals observed in healthy animals (Fig. 1b and 1d, S6) and 16 h after LPS challenge (Fig. 1b and 1d, S7). In the spectrum of liver tissue, both signals overlap with other naturally occurring liver signals. The subtraction of the signal observed in healthy animals (Fig. 1b and 1d, S6) from the signal observed in animals challenged for 16 h with LPS (Fig. 1b and 1d, S7) leads to a decrease in both NO–Hb and NO–Fe peaks, thus enhancing the overlapping with naturally occurring signals (Supporting Fig. S1). To find the optimum means of estimating the intensity of NO–Hb and NO–Fe signals, model signals of both species were analyzed.

NO–Hb signals were generated as a function of Hb concentration in the presence of an NO excess (Fig. 2). Different parameters of the spectrum were used to estimate the intensity of this signal: amplitude 1 (AMP1), amplitude 2 (AMP2), amplitude 3 (AMP3), and the double integral (DI). AMP1 and DI reflect both 5- and 6-coordinated NO–Hb complexes, while AMP2 corresponds to 5-coordinated heme iron and AMP3 to 6-coordinated heme iron, respectively. All four parameters showed linear correlation with Hb concentrations, suggesting that any of these parameters can be used for quantification of NO–Hb.

A similar picture was observed when an excess of Hb was treated with increasing concentrations of $NaNO_2$. Similarly, all four parameters showed a linear correlation with NO (nitrite) levels (Fig. 3). AMP1 slopes were similar in both cases. Because NO–Hb signal is generally represented by a sum of signals of 5- and 6-coordinated heme iron, the shape of the signals was analyzed. Thus, we calculated the ratio between the magnitudes (AMP1, AMP2, and AMP3) and DI, representing both complexes.

Figure 4 clearly shows that the shape of the signals does not change with increasing concentration of complexes, suggesting a constant ratio of 5- to 6-coordinated forms of Hb in the samples.

NO–Fe signals were generated and analyzed in the same manner (Fig. 5). This procedure must be performed in the natural tissue environment, because the shape and the position of the NO–Fe signal in the EPR spectrum depends on the nature of proteins donating SH groups to

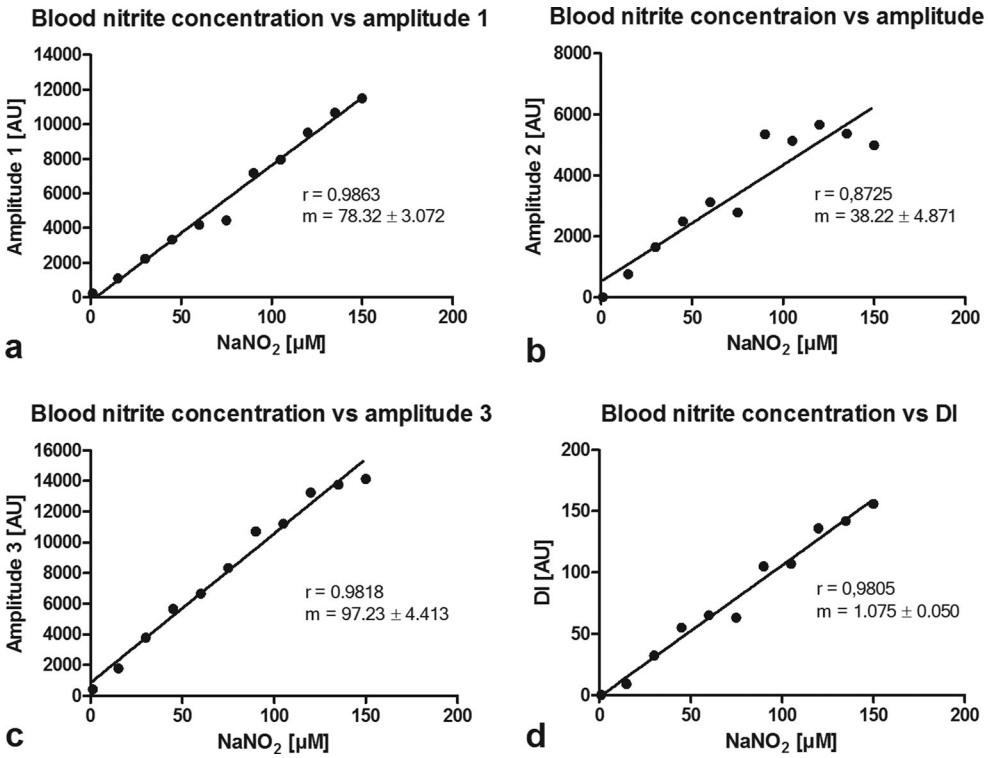

FIG. 3. Calibration curve for NO–Hb prepared using increasing nitrite ($NaNO_2$) concentrations (1–150 μM), 5 mM hemoglobin (Hb) and 50 mg dithionite per sample. We determined AMP1 (**a**), AMP2 (**b**), AMP3 (**c**), and the DI (**d**) of the NO–Hb signal as shown in Figure 2. Nitrite concentrations and intensity of NO–Hb signals show a strong positive correlation in case of all four quantitative parameters. Abbreviations: AMP, amplitude; m, slope; r, coefficient of determination.

form dinitrosyl–iron complexes. Therefore, liver homogenate was used for this calibration procedure. Liver homogenate, however, contains many other substances reacting with NO apart from Fe^{2+}. Consequently, the calibration of this signal using increasing NO levels was not possible, because a significant part of NO was trapped

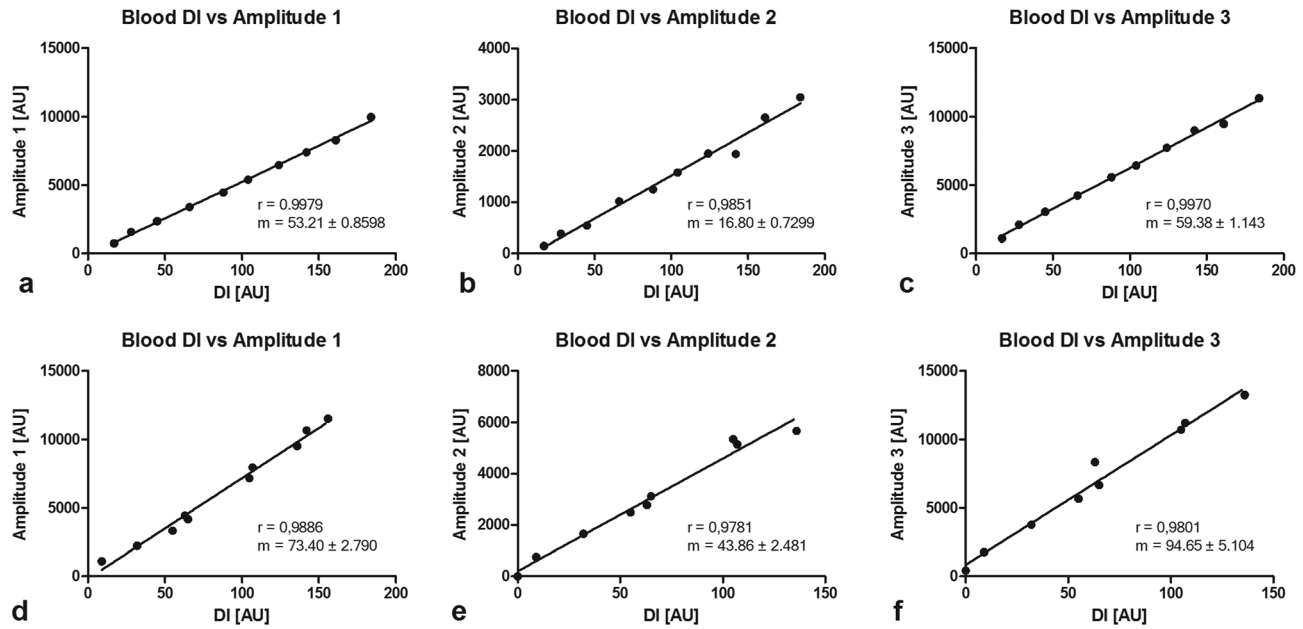

FIG. 4. Correlations between the NO–Hb quantification parameters provided by NO–Hb calibration based on variation in concentration of Hb (**a**–**c**) and nitrite (**d**–**f**) in the range of 1 to 150 μM. Strong correlations between AMP1 (a, d), AMP2 (b, e), AMP3 (c, f), and the DI indicate that the shape of the signal does not change at various concentrations of NO–Hb, regardless of whether Hb or nitrite concentrations were varied. Abbreviations: AMP, amplitude; m, slope; r, coefficient of determination.

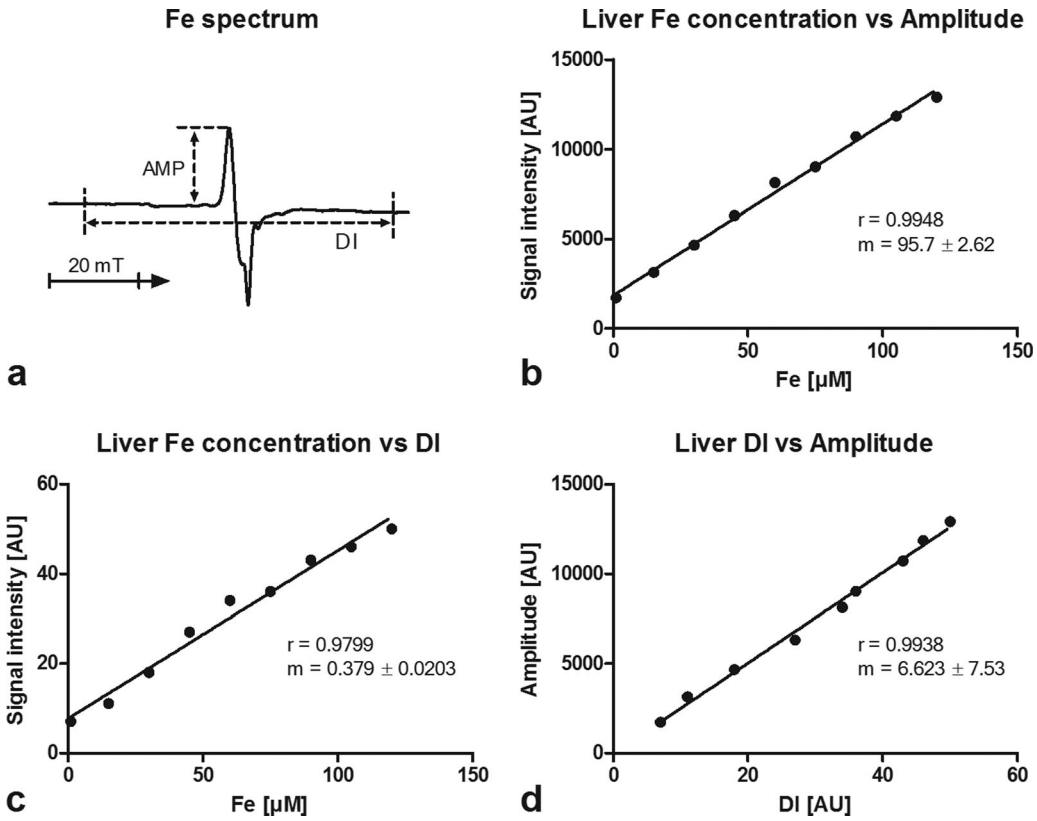

FIG. 5. Calibration of NO–Fe using 1 to 130 μM Fe(II)SO_4 and 1 mM nitrite in liver homogenate. The EPR spectra recorded in such NO–Fe calibration samples (**a**) provide two different quantification parameters: AMP and the DI (the range of integration is shown in the figure). The strong positive correlation between AMP and Fe(II)SO_4 concentration (**b**), as well as between DI and Fe(II)SO_4 concentration (**c**), shows that both parameters are suitable for NO detection. The good correlation between AMP and DI (**d**) shows that the shape of the signal does not change. Abbreviations: AMP, amplitude; m, slope; r, coefficient of determination.

by other species than Fe^{2+} (data not shown). To overcome this limitation, a different approach was necessary. For this, the signal was calibrated with increasing Fe^{2+} concentrations in the presence of an excess of NO, similarly to the calibration of NO–Hb signal with increasing Hb concentrations. This method delivered clear NO–Fe signals (Fig. 5a), which were analyzed by determining the intensity (amplitude, AMP) and the DI (Fig. 5). Both parameters showed a strong correlation with Fe^{2+} concentrations as well as with each other.

To quantify NO–Hb and NO–Fe in liver tissue, the magnitudes of parameter AMP1 of NO–Hb signal and parameter AMP of NO–Fe signal were chosen because they were the most distinguishable in the complex EPR spectrum of the liver. These selected parts of signals and the corresponding calibration curves were used to determine intra- and extracellular NO concentrations in liver and circulating arterial blood of animals subjected to bacterial endotoxin (Fig. 6b). NO–Hb in blood and NO–Fe in liver correlated with the LPS doses (Fig. 6c–6e). Furthermore, all three parameters correlated well with each other (Figure 6f–6h).

The signal-to-noise ratio is a measure of the sensitivity. Absolute sensitivity threshold is commonly defined as a concentration of a substance needed to get a signal equivalent to the noise observed in the spectrum. However, in our samples, the minimal signal-to-noise ratio allowing the evaluation of NO-related signals in liver biopsies was 3. On the basis of this value, we determined the sensitivity of the method for NO–Fe and NO–Hb complexes. We assessed the instrumental noise by measuring its amplitude in sections of spectra where no specific signal was present. Detection limit of the method is 0.61 nmol/cm^3 for NO–Hb and 0.52 nmol/cm^3 for NO–Fe.

DISCUSSION

Here we demonstrate the possibility of determining levels of NO generated in blood and tissue compartments of liver in a single liver biopsy. This method is based on the fact that Hb, a strong scavenger of NO, is located exclusively in blood, and that blood plasma does not contain free Fe^{2+}, because in blood they are all oxidized by ceruloplasmin and bound to transferrin (Fig. 7). In contrast, parenchymal cells (eg, hepatocytes) contain Fe^{2+} but do not contain Hb. Consequently, NO occurring in blood will be trapped by Hb yielding NO–Hb complexes, whereas NO generated inside the liver cells will be bound to Fe^{2+} to form NO–Fe complexes. Both complexes have distinct EPR spectra (Fig. 1b and 1d, S8 and S9). Hepatocytes contain certain amounts of heme proteins, which theoretically can form NO–Hb complexes, thus limiting the method described here. However, our experiments showed that liver perfused with Ringer's solution displays an NO–Fe signal

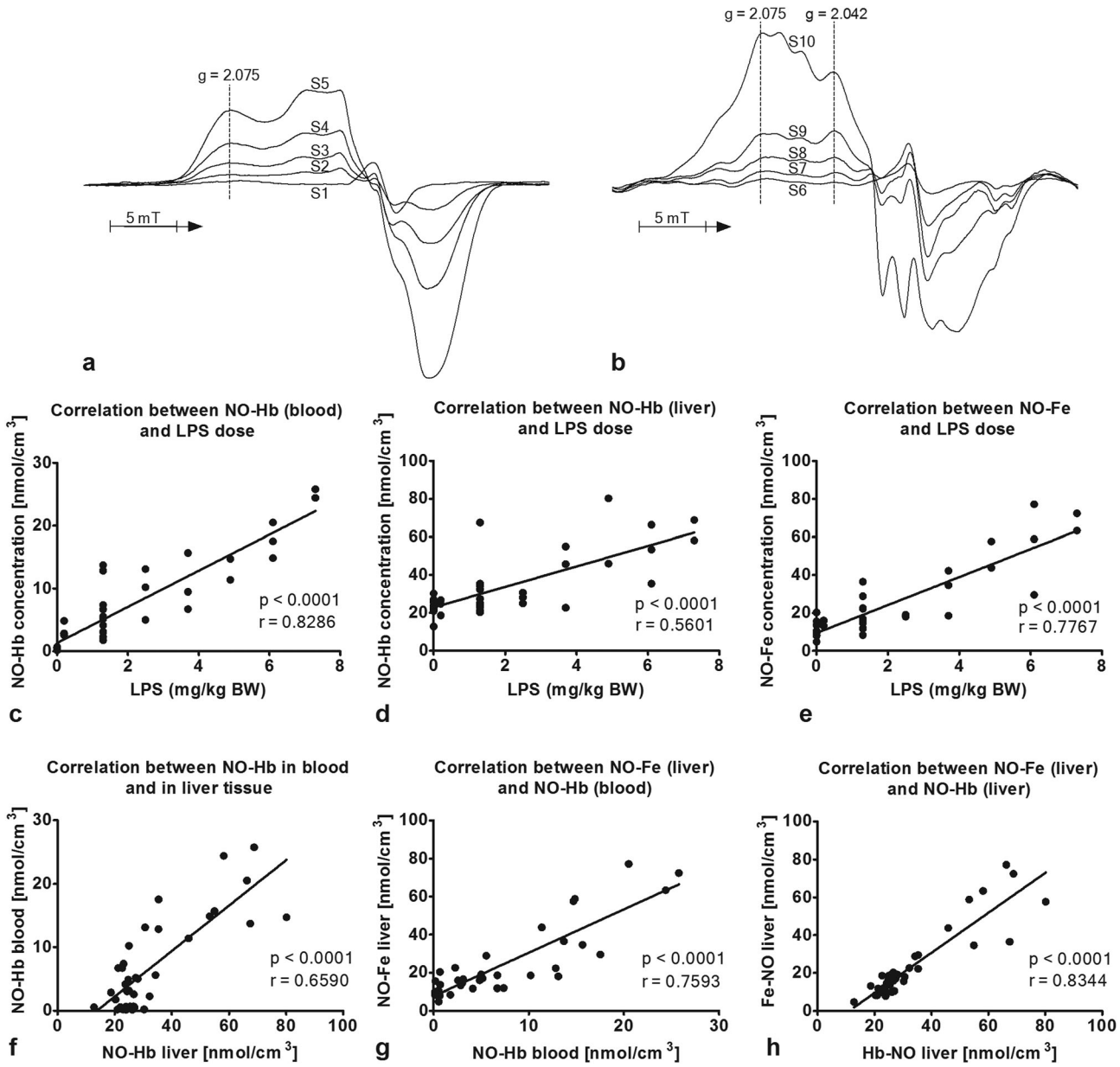

FIG. 6. Quantification of NO formed in cells and in blood upon LPS treatment and characterization of NO pools. The dose of LPS varied from 0.2 to 7.3 mg/kg body weight. Blood (**a**) and liver (**b**) EPR spectra were recorded 16 h after injection of 0.2 (S2, S7), 3.7 (S3, S8), 4.9 (S4, S9), and 8.5 (S5, S10) mg/kg body weight LPS or an equivalent volume of NaCl (S1, S6). NO–Hb in blood (**c**) and liver (**d**), as well as NO–Fe in liver tissue (**e**) correlated with LPS dose. There was also a good correlation between all these parameters (**f–h**). Abbreviations: m, slope; r, coefficient of determination; S, signal.

exclusively, whereas nonperfused liver has both NO–Hb and NO–Fe signals. On this basis, we developed a method that allows the determination of both paramagnetic signals in a single EPR spectrum of frozen liver samples.

An important aim of this study was quantification of the signals. We tested different approaches to create calibration curves for the quantification of NO-related signals in liver spectra.

In a test tube, we varied concentrations of either natural NO traps (Hb and Fe^{2+}) or NO reduced from nitrite (Figs. 2 and 5). We showed that the most feasible way of calibration is the variation of NO trap (Hb and Fe^{2+}) concentrations in the presence of an excess of NO. Using this calibration method, it was possible to avoid artifacts due to the formation of complexes other than nitrosyl complexes, as well as oxidation of NO to other nitrogen species.

Quantification of NO-related signals in blood and liver of rats after intravenous endotoxin treatment revealed that the highest NO concentrations occurred in blood of liver vasculature, the second highest NO levels were observed in intracellular compartments, and the lowest concentration was found in circulating blood (Fig. 6).

These data indicate that the liver is an important source of NO found in circulating blood. It should be noted, however, that the mesenteric system may also contribute to elevated NO levels during inflammation (9).

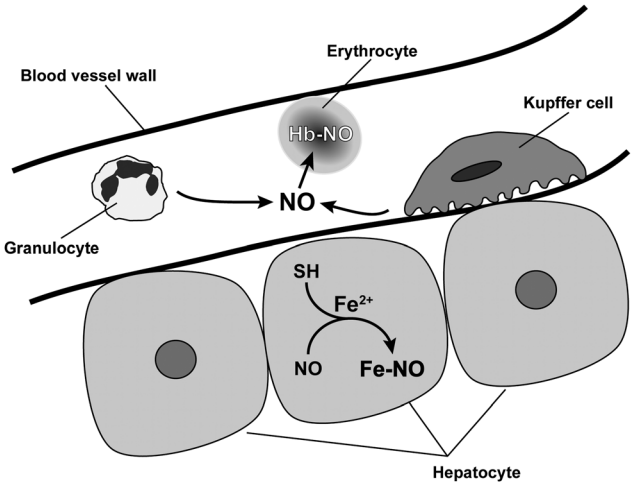

FIG. 7. Endogenous traps of NO inside parenchymal cells and small blood vasculature of the liver. After being synthesized by hepatocytes, NO is trapped by ferrous ions (Fe^{2+}) from the cytosolic free iron pool, which forms a dinitrosyl–iron complex (NO–Fe) with two NO molecules and two thiol groups of proteins (SH). We assume that a small fraction of the NO molecules synthesized in hepatocytes diffuses into the microvasculature, where together with the NO molecules synthesized by immune cells (granulocytes, Kupffer cells) forms mononitrosyl–hemoglobin complexes (NO–Hb). This scheme shows that NO–Hb complexes predominantly reflect extracellular NO generation by immune cells, whereas NO–Fe is a matter of intracellular NO synthesis.

Kupffer cells may be the other substantial source of NO detectable in blood compartment of the liver (Fig. 7). In a previous study, we showed that NO is able to diffuse from tissues to blood, but not vice versa (13). These findings explain the high correlation between NO–Hb and NO–Fe in nonperfused liver, which was stronger than the correlation between NO–Hb in blood and liver. This finding suggests that NO formed in liver cells diffuses into the blood compartment (microvasculature of liver) and is subsequently bound to Hb.

NO–Hb is present in two forms in mammals: 5-coordinated and 6-coordinated heme-iron complexes, which have distinct EPR spectra (14). According to Fink et al. (15), animal (rodent) NO–Hb exists predominantly in the 5-coordinated form, whereas human NO–Hb exists predominantly in 6-coordinated complexes.

In our model, the formation of NO–Hb complexes in the blood compartment of the liver may be indirectly confirmed by the fact that NO–Hb complexes in blood were mostly 6-coordinated (Fig. 6a), whereas the 5-coordinated form of NO–Hb was more dominant in liver tissue (Fig. 6b), suggesting that these complexes do not originate in blood. Therefore, for the evaluation, we selected a part of the spectrum in which the signals of both the 5- and 6-coordinated forms were present.

Our data suggest that dinitrosyl–iron complexes scavenge only a part of NO formed in cells, whereas the other part can contribute to physiological NO signaling and/or diffuse into the blood. This conclusion can be drawn from a comparison of our data with NO concentrations determined in the tissue using the specific NO trap iron-diethylthiocarbamate in a similar model, where these values were substantially higher (16).

CONCLUSIONS

The proposed method enables the specific quantification of intra- and extracellular NO levels in liver biopsies by analyzing the NO–Hb and NO–Fe signals. These naturally occurring NO complexes have distinct EPR spectra and act as endogenous NO traps, wherefore they represent an excellent alternative for the potentially harmful exogenous NO traps. From our experiments it emerged very clearly that the NO–Fe complexes detected in liver tissue are formed only in parenchymal compartment, whereas the NO–Hb complexes detected in both, blood and unperfused liver tissue, are formed only in blood compartment. This finding together with the observation that NO–Hb is no longer detectable in liver tissue after removal of RBCs by tissue perfusion reinforces the statement that NO–Fe occurs exclusively in parenchymal cells and NO–Hb in blood, emphasizing the usage of NO–Fe and NO–Hb signals to distinguish between intracellular and extracellular NO levels. In addition, the coordination state of NO to Hb, which is delivered with the same EPR spectra, allows a further distinction between the NO–Hb complexes formed within liver and nonliver vasculature. Accordingly, NO–Hb complexes detected in blood are mainly 6-coordinated, whereas those detected in liver vasculature are mainly 5-coordinated.

Despite the decrease in sensitivity, the detection method based on endogenous NO traps has an advantage in that it interferes less with metabolic pathways of NO. The major advantage, however, is that it does not require any injection of NO traps. The latter enables to use this assay in clinical settings. Thus, our study provides a viable method and simultaneously underlines the necessity to examine human biopsies. As a first step, retrospective analysis of samples kept in the bio banks should be performed.

ACKNOWLEDGMENTS

The authors thank Tanja Stögerer for technical support and Carina Penzenstadler for animal handling.

REFERENCES

1. Bryan NS, Bian K, Murad F. Discovery of the nitric oxide signaling pathway and targets for drug development. Front Biosci (Landmark Ed) 2009;14:1–18.
2. Forstermann U, Sessa WC. Nitric oxide synthases: regulation and function. Eur Heart J 2012;33:829–837, 837a–837d.
3. Nicholson S, Bonecini-Almeida MG, Lapa e Silva JR, et al. Inducible nitric oxide synthase in pulmonary alveolar macrophages from patients with tuberculosis. J Exp Med 1996;183:2293–2302.
4. Wei XQ, Charles IG, Smith A, Ure J, Feng GJ, Huang FP, Xu D, Muller W, Moncada S, Liew FY. Altered immune responses in mice lacking inducible nitric oxide synthase. Nature 1995;375:408–411.
5. Wong JM, Billiar TR. Regulation and function of inducible nitric oxide synthase during sepsis and acute inflammation. Adv Pharmacol 1995;34:155–170.
6. van Faassen EE, Bahrami S, Feelisch M, et al. Nitrite as regulator of hypoxic signaling in mammalian physiology. Med Res Rev 2009;29:683–741.
7. Lundberg JO, Gladwin MT, Ahluwalia A, et al. Nitrate and nitrite in biology, nutrition and therapeutics. Nat Chem Biol 2009;5:865–869.
8. Knott AB, Bossy-Wetzel E. Nitric oxide in health and disease of the nervous system. Antioxid Redox Signal 2009;11:541–554.
9. Boveris A, Valdez L, Alvarez S. Inhibition by wine polyphenols of peroxynitrite-initiated chemiluminescence and NADH oxidation. Ann N Y Acad Sci 2002;957:90–102.
10. Gow AJ, Stamler JS. Reactions between nitric oxide and haemoglobin under physiological conditions. Nature 1998;391:169–173.

11. Gow AJ, Luchsinger BP, Pawloski JR, Singel DJ, Stamler JS. The oxyhemoglobin reaction of nitric oxide. Proc Natl Acad Sci U S A 1999; 96:9027–9032.
12. Sergent O, Tomasi A, Ceccarelli D, Masini A, Nohl H, Cillard P, Cillard J, Vladimirov YA, Kozlov AV. Combination of iron overload plus ethanol and ischemia alone give rise to the same endogenous free iron pool. Biometals 2005;18:567–575.
13. Kozlov AV, Sobhian B, Costantino G, Nohl H, Redl H, Bahrami S. Experimental evidence suggesting that nitric oxide diffuses from tissue into blood but not from blood into tissue. Biochim Biophys Acta 2001;1536:177–184.
14. Dikalov S, Fink B. ESR techniques for the detection of nitric oxide in vivo and in tissues. Methods Enzymol 2005;396:597–610.
15. Fink B, Dikalov S, Fink N. ESR techniques for the detection of nitric oxide in vivo as an index of endothelial function. Pharmacol Rep 2006;58(Suppl.):8–15.
16. Kozlov AV, Albrecht M, Donnelly EM, Jafarmadar M, Szelenyi Z, Nohl H, Redl H, Bahrami S. Release and hemodynamic influence of nitro-glycerine-derived nitric oxide in endotoxemic rats. Vascul Pharmacol 2005;43:411–414.

SUPPORTING INFORMATION

Additional Supporting Information may be found in the online version of this article.

Fig. S1. EPR spectra obtained from sham-operated animals (S1) and animals challenged with 6.3 mg/kg body weight of LPS for 16 h (S2). Both spectra show the NO–Hb and NO–Fe peaks, which arose at $g = 2.075$ and $g = 2.042$, respectively. The subtraction of S1 from S2 (S3) led to a decrease in both peaks, making it more difficult to observe and quantify them. Abbreviations: g, g-factor; S, signal.